Solar thermal treatment of non-metallic minerals: The potential application of the SOLPART technology

Cite as: AIP Conference Proceedings **2126**, 180002 (2019); https://doi.org/10.1063/1.5117682
Published Online: 26 July 2019

Jan Baeyens, Huili Zhang, Weibin Kong, Philippe Dumont, and Gilles Flamant

Solar Thermal Treatment of Non-Metallic Minerals: the Potential Application of the SOLPART Technology

Jan Baeyens[1, 2, a)], Huili Zhang[2, b)], Weibin Kong[2, c)], Philippe Dumont[3, d)], Gilles Flamant[4, e)]

[1]*European Powder and Process Technology, Park Tremeland 9, 3120 Tremelo, Belgium*
[2]*Beijing University of Chemical Technology, School of Life Science and Technology,15# Beisanhuan east road, Beijing, China*
[3]*New Lime Development, Rue Warfusée 78, St. Georges-sur-Meuse, Belgium*
[4]*Promes-CNRS, Rue du Four Solaire 7, 66120 Font Romeu, France*

[a)]europpt@gmail.com
[b)]zhhl@mail.buct.edu.cn
[c)]kongweibin2012@gmail.com
[d)]ph.dumont@forlime.be
[e)]Corresponding author: Gilles.Flamant@promes.cnrs.fr

Abstract. The solar horizontal bubbling fluidized bed concept developed within the SOLPART research project can be used as a solar receiver-reactor. This application offers a considerable industrial potential, as illustrated in the paper further to different experiments and industrial contacts. The most demanding application is the calcination of limestone, either as pure calcite, or as 85% mix in cement raw meal. The decomposition temperature exceeds 850 °C (nearly the application limits of refractory steel alloys). Other calcinations (e.g. dolomite, gypsum, phosphate rock, meta-kaolin, clays, etc.) are less demanding since occurring at a lower calcination temperature and with an endothermic reaction heat that is significantly lower than the reaction heat of $CaCO_3$, which is therefore considered as a relevant test case.

BACKGROUND AND CONTEXT

SOLPART is the acronym of a European Union's H2020-funded research programme that targets the solar processing of reactive particles. Several minerals require a physical-chemical and thermal treatment prior to their application as mineral feedstock and use in the production of value-added products. The thermal processes are energy-consuming, partly due to the preheating of the minerals to their reaction temperature, but mostly due to the endothermic reaction itself. Limestone is the major mineral to be considered, as feedstock in the lime and cement industries, but also as substantial and dominant compound of dolomite, and the contaminant to be calcined in phosphate ore. The investigated solar decomposition of minerals can be expanded to other products, albeit of secondary importance. Phosphate ore, gypsum, clays, kaolinite are among these secondary objectives, as illustrated in Table 1 below. The required treatment temperature of reactions that produce CO_2 are determined by the equilibrium calculations involving the Gibbs free energy, and hence by the partial pressure of CO_2 (P_{CO2} in Table 1) in the reactor environment.

As shown in the Table, the processes are energy-intensive, implying the use of significant quantities of fossil fuels. The total consumption energy in the target lime production processes is in the range of 3600 – 5000 kJ/kg of CaO, and in the range of 3100 – 4200 kJ/kg of clinker (cement industry) and represents 40% of the total production cost per ton of cement (dry rotary kiln with cyclonic pre-heaters) and up to 60% in the case of lime kilns [1]. If fossil fuels are used, about 40% of the total CO_2 emission from lime industry production relates to the combustion and 60% relates to the reaction itself. Substituting fuel by concentrated solar energy may result in up to 40% reduction of CO_2

SolarPACES 2018
AIP Conf. Proc. 2126, 180002-1–180002-8; https://doi.org/10.1063/1.5117682
Published by AIP Publishing. 978-0-7354-1866-0/$30.00

emission in the lime industry. Since in the cement industry a high temperature sintering follows the pre-calcination process, the total reduction is about 20%. In the thermal treatment of phosphate ores and other minerals, the CO_2 emission from the reactions is less outspoken, since the carbonate content is far lower than in lime or cement raw meal,. CO_2 emission from fuel combustion is eliminated by using solar energy, representing e.g. 6.5 kg CO_2/ton phosphate.

TABLE 1. Conditions and objectives of thermal treatments of target minerals

Reaction system	T (°C)	Sensible heat reqd. kJ/kg of product	Reaction heat kJ/kg of product	Use
$CaCO_3 \rightarrow CaO + CO_2$	850-950 f(P_{CO2})	500 to 2000, function of degree of heat recovery	3000-3200	Lime, Cement
$MgCa(CO_3)_2 \rightarrow MgO.CaO + 2CO_2$	650-750 f(P_{CO2})	See above	2400-2700	Dolomite, Dolomitic Lime
Meta-kaolinite	550-900	300 to 500, function of degree of heat recovery	~700	Pozzolanic additive for cement and lime-mortar
Phosphate ore	700-1000	Max. 300, function of degree of heat recovery	Exothermic (combustion of C-contaminants); Mostly endothermic (calcite calcination)	Feed stock for Phosphate Industry
Clays, Sands with organic contaminants	600-700	~700	Slightly exothermic by combustion of organic contaminants	Ceramics, Pipes, Tiles, Concrete

THE TARGET PARTICLES

SOLPART intends to decompose non-metallic minerals by concentrated solar irradiance of a fluidized bed reactor. Two different types of particles will be treated, i.e. free-flowing and cohesive particles. This is already evident from the particle size, when the Sauter means particle size is considered, being ≤ 10 µm for cement raw meal (CRM), 50-130 µm for limestone and dolomite, and < 350 µm for milled phosphate and other ores. The combination of mean particle size and density of most of the minerals and their products (e.g. CaO from $CaCO_3$) classifies them as Geldart A or B-type powders, easily handled, stored, discharged and conveyed [2]. It should be remembered that the Geldart powder classification distinguishes C (cohesive), A (aeratable), B (bubbling) and D (coarse) particles. At an absolute particle density of 2600 kg/m³, cohesive powders have a particle size below ~ 35 µm; aeratable powders range between 35 and ~100 µm; B-type powders have a particle size between ~100 and 450 µm, whereas the particle sizes of coarse or D-type powders exceed 450 µm. CRM is even visually seen as highly cohesive. This cohesiveness was hence examined in detail at temperatures between 20 and 850 °C according to various criteria, being (i) the Geldart classification C/A; (ii) the Hausner ratio = $\rho_{tapped}/\rho_{loose;}$ with ρ_{loose} and ρ_{tapped} the bulk density of the powder in its loose or tapped state, respectively [2]; (iii) the yield stress as a result of consolidation vs. shear; (iv) the Angle of Repose (AoR); and (v) the balance of forces.

A Hausner ratio in excess of 1.25 is characteristic for a cohesive powder. Results clearly illustrate the difference between CRM and e.g. 58 µm limestone, with values for CRM ranging from 1.25 to 1.38, against 1.05 for limestone. Bulk densities are moreover slightly higher at higher temperature, meaning that the powder is more consolidated, with typical values of 1191 kg/m³ (850°C) and 1078 kg/m³ (20°C) for CRM, and 1560 kg/m³ (850°C) against 1492 kg/m³ (20°C) for 58 µm limestone.

The Angle of Repose [3] provides additional information and was determined in an electrical furnace by pouring the powders on a flat plate and measuring the angles of the slopes. Criterion of assessment are: AoR < 30 (flowable); AoR 30 - 45 (some cohesiveness); AoR 45 - 55 (true cohesiveness) and AoR > 55 (high cohesiveness, limited flowability). Results are again confirming the cohesiveness of CRM, with AoR increasing from 62-65° at 20°C, to 70-72° at ~850°C. Limestone values vary from 27° at 20°C to 31° at ~800°C.

Initially developed by Baeyens et al. [4], a total force balance for the powder behaviour can be established. Whereas the CRM powder will be characterized by very strong Van der Waals cohesive forces, coarse particles such as limestone-lime will show no cohesiveness.

The experimental work on the Yield limit [5] assesses the effect of the consolidation on the incipient flow. The flow factor ratio $ff_c = \sigma_1/\sigma_c$ characterizes the flowability of bulk solids, where greater values of the ratio represent a greater flowability of the powder. σ_1 is the normal consolidation stress, whereas σ_c is the stress at failure. The numerical classification is the following [Schulze]: $ff_c < 1$ (non-flowing); $1 < ff_c < 2$ (very cohesive); $2 < ff_c < 4$ (cohesive); $4 < ff_c < 10$ (easy-flowing); and $10 > ff_c$ (free-flowing). Results obtained in a shear cell at different temperatures provide results. With a $ff_c \leq 2$, CRM is considered very cohesive. Limestone and dolomite have a $ff_c > 10$, and are freely flowable. It can hence be concluded that limestone/dolomite and other A/B-type minerals pose no problem, since perfectly flowable, whereas CRM is cohesive to very cohesive according to all criteria. Shear is needed (air flow) to reduce the cohesive Van der Waals forces, and this explains the use of a lean phase pre-calciner and aerated CRM storage silos.

REACTION THERMODYNAMICS AND KINETICS

Not only the data at thermodynamic equilibrium are important, but also the kinetics, i.e. the rate of progress of the reaction needs to be considered, since it must be compatible with the required reactor design.

The schematic of the reactions is illustrated in Fig. 1. High grade heat is converted into chemical energy by promoting an endothermic reaction of compound A, whereby reaction product B is obtained, and reaction product C (mostly a gas or vapour) is either stored for further re-use or exhausted. An inert gas can be used to help removing components C from the reaction mixture.

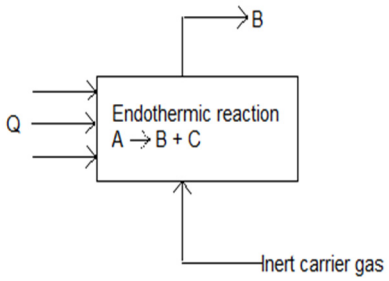

FIGURE 1. Schematic of the minerals' decomposition reaction

Towards **thermodynamics of the systems**, various parameters are important. The amount of heat needed is proportional to the amount of material (m), the endothermic heat of the reaction (ΔH_r) and the conversion (α), given by

$$Q = m\alpha\Delta H_r, with \quad \alpha \leq 1 \tag{1}$$

The total heat to be applied will exceed ΔH_r, since also the sensible heat of reactant A will need to be supplied between its initial temperature and the reaction temperature, hence with an important influence on the overall heat efficiency. The thermodynamic criteria for the preliminary screening of candidate reactions are assessed from available thermodynamic equilibrium data with two essential parameters.

The first is the "turning" or equilibrium temperature, T_{eq}, defined as the temperature at which neither forward nor reverse reactions are thermodynamically favoured. T_{eq} is derived by applying the definition of the Gibbs' free energy to the condition of T_{eq}.

$$\Delta G(T_{eq}, P) = 0 \tag{2}$$

where ΔG is the Gibbs' free energy change for the reaction, simplified as $\Delta G = \Delta H - T\Delta S$, in this case

$$T_{eq} = \frac{\Delta H(T_{eq}, P)}{\Delta S(T_{eq}, P)} \tag{3}$$

with ΔH and ΔS respectively the system enthalpy and entropy at pressure P and temperature T_{eq}. The reaction entropy is positive for the decomposition, and of equal value but negative for the reverse reaction.

The second screening parameter is the heat of reaction ΔH_r, expressed in kJ/kg of reactant, and determined by the free energy of formation and the Kirchhoff's law. From the calculations, Table 2 illustrates both screening parameters for the selected reaction pairs.

TABLE 2. Possible reaction pairs

Reaction A ↔ B + C (+D)	C_p (of A) [kJ/kgK]	T_{eq} (P=1 atm) [°C]	ΔH_r at T_{eq} [kJ/kg of A]
$CaCO_3 \leftrightarrow CaO+CO_2$	$0.8227+0.000497T-12{,}858.72/T^2$	839	1703
$MgCO_3 \leftrightarrow MgO+CO_2$	0.8387	303	1126
$CaMg(CO_3)_2 \leftrightarrow CaO+MgO+2CO_2$	0.92	490	868

For cement raw meal, as a mixture of ~85% of limestone, and 15% of alumina-silicates, the specific heat is about 1.05 kJ/kgK. The equilibrium temperature is ~839 K, and the reaction heat is ~1659 kJ/kg.

In the lower ranges of partial CO_2 pressures, as often representative of the calcination reactions where reaction gases or vapours are vented to the atmosphere, the effect of pressure-induced changes of T_{eq} is significant, even of the order of 100 K at very low values of P. Only at high partial pressures does the value of T_{eq} remain nearly constant.

For conversion, both **reaction kinetics and residence time** in the reactor environment need to be assessed. For operation with a continuous feed of solids, the exit stream consists of particles of different ages and degrees of conversion. The average conversion of this stream is thus dependent upon (i) the rate of reaction of single particles in the reactor environment, and (ii) the residence time distribution of solids in the reactor.

The conversion of solids can follow one of two extremes of behaviour. At one extreme, heat diffuses rapidly enough into the particle so that the reaction is more or less uniform throughout the particle. At the other extreme, diffusion is so slow that the reaction zone is restricted to a thin front which advances from the outer surface into the particle. Real situations lie somewhere between both extremes. According to the step that is rate-controlling, different kinetic expressions are obtained. The detailed derivation of the expression is given elsewhere [6]. The conversion equations are usually expressed in terms of a characteristic time τ, the time to completely convert an unreacted particle into product. For fine particles (≤ ~200 μm), diffusion is not important, and the reaction rate controls the reaction kinetics [7–10]. Since the decomposition must proceed against combustion gases and the CO_2 generated by the decomposition, the decomposition time τ will increase and will approach ∞ for conditions of temperature where the equilibrium pressure P_{EQ} is lower than the real partial CO_2 pressure of the calcination environment. It is therefore necessary to apply a correction coefficient so that:

$$\tau' = K_c \tau, with\ K_c = \frac{1}{1 - \frac{P_{CO2}}{P_{EQ}}} \tag{4}$$

Most of the data are moreover established for spherical particles. In practice, no limestone or mineral is perfectly spherical and its shape depends largely on the nature of the deposit, the type of crusher used, the sieving etc. The shape of the particle is very important for reaction kinetics and heat transfer. It is to be expected that a flake or a rod will decompose faster than the equivalent volume sphere of limestone and this affects the required time for complete decomposition, τ. In practice, the τ values must be corrected both for operation CO_2 pressure (K_C) and limestone shape (K_S) and result in

$$\tau^* = K_S K_C \tau \tag{5}$$

Wührer[11] indicates shape coefficient K_S as 0.83 for cubes and 0.44 for rods.

It should however be remembered that the flowability of flakes and rods will be reduced in comparison with the flow-behavior of spheres.

KINETICS FROM EXPERIMENTAL INVESTIGATIONS

The target reactions were examined by thermogravimetry, measuring the weight loss of the sample, recording the initial sample weight (M_0), the sample weight at time t (M_t) and the weight of the sample after completion of the thermal decomposition (M_∞). The conversion α is calculated as

$$\alpha = (M_0 - M_t)/(M_0 - M_\infty) \quad (6)$$

The reaction rate constant can be derived within the complete time and/or temperature scale, as described in detail for other chemical processes by Brems et al.[12]. Since α is the conversion, the relative amount of feed left at any time is (1- α). The assumption is made that the reaction rate constant follows the Arrhenius equation:

$$k = A\exp(\frac{-E_A}{RT}) \quad (7)$$

In this equation k is the reaction rate constant (is s^{-1} for a first order reaction), A the pre-exponential factor (same units as k), E_A the activation energy (J/mol), R the universal gas constant (8.314 J/molK) and T the temperature (K).

The rate of degradation, $d\alpha/dt$ is a function of the T-dependent rate constant k, and a function of the T-independent conversion $f(\alpha)$ [12].

For a first order reaction, the conversion expression is

$$ln(1-\alpha) = -kt = -A\exp(\frac{-E_A}{RT}) \quad (8)$$

For a second order reaction, the conversion expression is

$$[(1-\alpha)^{1-2} - 1] = -A\exp(\frac{E_A}{RT}) \quad (9)$$

Within the various models used, models with n of 1 or 2 resulted in R^2-values in excess of 0.994 and 0.923, respectively. Other reaction rates (n= 0.5, > 2) provided R^2 values below 0.7. It is hence concluded that the reaction rate expression with order of reaction 1 provides a fair approach to the different reactions. From the first order kinetics, the values of the activation energy and of the pre-exponential factor were determined, and are given in Table 3, allowing the prediction of the kinetic rate constant, k, at any temperature by using the Arrhenius equation.

TABLE 3. 1st-order reaction results for different reactions.

Reaction	E_A [kJ/mol]	A [s^{-1}]
$CaMg(CO_3)_2 \leftrightarrow MgO+CaO+2CO_2$	219	1.15×10^{12}
$CaCO_3 \leftrightarrow CaO+CO_2$	228	7.03×10^{7}
Cement raw meal	224	6.53×10^{7}

To achieve 95 % of the maximum conversion in a first order reaction, the required reaction time at T_{eq} indicates that the reactions can be completed for fine particles in less than a minute. This is however tentative only, and pilot/large scale experimentation is certainly required.

MASS AND ENERGY BALANCES

The mass balances determine the feed rate (kg/h) of raw material for the given target production, respectively 5 kg/h in lab-scale, and 30 kg/h in pilot-scale for the SOLPART project. Lab-scale values are given in Table 4.

TABLE 4. Mass balance of the lab-scale solar reactor (5 kg/h output, 95% conversion)

$CaCO_3$	**$CaCO_3$: 9.2 kg/h**	**CaO: 5 kg/h ; $CaCO_3$: 0.3 kg/h; CO_2: 3.9 kg/h**
Dolomite	Dolomite: 9.8 kg/h	CaO.MgO: 5 kg/h; Dolomite: 0.2 kg/h ; CO_2: 4.6 kg/h
CRM	CRM: 8.3 kg/h	CaO + "inerts": 5 kg/h ; CO_2: 3.3 kg/h

The maximum heat to be supplied, based upon the mass balance includes the sensible heat of the limestone feed, the sensible heat of the fluidization air, and the reaction heat. A total of 17785 kJ/h, or 4.9 kW is required. For the pilot scale application, all values are multiplied by 6, leading to a net required heat supply of 29.6 kW.

SELECTED SOLAR REACTOR TECHNOLOGY

Different types of solar reactor were tested in the framework of the SOLPART project. both the Upflow Bubbling Fluidized Bed (UBFB) [13–15] and a solar rotary kiln[16] were initially tested. Problems of dust formation, difficulties to meet the required residence in a single pass operation, the effect of high CO_2 partial pressures in the reactor environment, and the cohesiveness of some of the required raw materials were major drawbacks.

A shallow cross-flow bubbling fluidized bed (CfBFB) was hence developed by the Beijing University of Chemical Technology (BUCT) in collaboration with European Powder and Process Technology (EPPT) and PROMES-CNRS.

Industrial fluidized beds are mostly of the "well-mixed" type. Due to the near perfect mixing, the bed has close to a uniform composition and temperature, equal to the outlet stream in a continuous operation. Fluidization gas also exits the bed at bed temperature. Despite the good mixing of feed particles within the bed, the main disadvantage is the residence time distribution leading to a distribution in product characteristics since about 40% of the particles stay in the bed for less than half of the average residence time, $\bar{t}$, and about 10% for less than one-tenth of $\bar{t}$.

Where strict product properties are required, where a temperature gradient from feed to discharge is desired, or where the pressure drop across the bed needs to be limited, the use of continuous cross-flow fluidized beds can be applied. Particles flow along a channel of high length/width radio, and the objective is to approach plug flow of the particles with a near-equal residence time. Straight channel designs are often provided with baffles normal to the direction of particle flow to further enhance plug flow. In addition to having a narrow spread on residence time and product properties, a plug flow bed will normally require a smaller bed volume than a well-mixed bed to achieve the same performance [17]. Shallow beds moreover have a low bed pressure drop. The single stage cross-flow fluidized bed is tentatively presented in Fig. 2. As in the UBFB case, parasitic losses (pressure drop, amount of sensible heat loss with fluidizing gas), the required high flow rate of fluidization gas, and large size of equipment will be limited by using Geldart group A-powders.

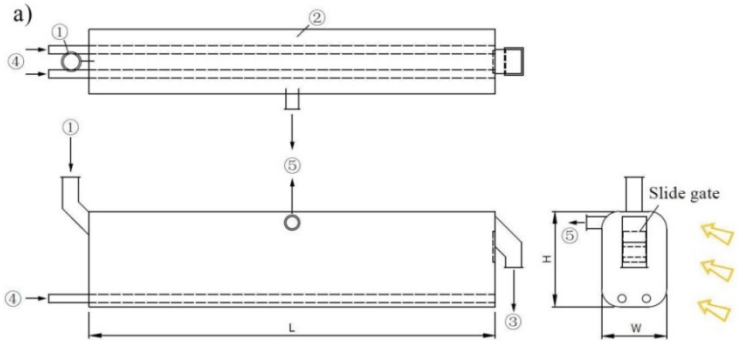

FIGURE 2 Illustration of a cross-flow bubbling fluidized bed: (a) in a solar thermal application [18] with ① feed of particles, ②horizontal fluidized bed, ③ discharge of particles, ④ multi-orifice air distributors, ⑤ exhaust air.

First experiments on lab-scale, using dolomite, gypsum and mete-kaolinite were completed and prove that the required conversion can be obtained in a single pass operation. Results with limestone are ongoing.

MARKET PROSPECTS

Calcination of Limestone, Dolomite and CRM

The limestone-lime market outside China is dominated by 2 international groups, i.e. Carmeuse and Lhoist. Whereas Lhoist is mostly active in Europe (limited solar potential), Carmeuse has production facilities in Europe, in the Middle and Far East, in Africa, in the USA and in South America. Carmeuse offers several options for joint development of the technology in Italy (Carrara), Turkey (4 plants), Oman, Florida, and Colombia. An initial study for a 40 ton/day plant for both limestone and dolomite was conducted for the Carmeuse Soma-site in Turkey, where the solar irradiance pattern is excellent outside the winter season. The study demonstrated that a hybrid solar-biomass kiln offers a high potential. Investments were estimated, with costs of 1.9 M€ (Heliostats and solar tower), 1.3 M€ (Calcination reactor, cooling and preheating) and 0.65 M€ (Site layout, utilities). The calculated production cost of quicklime was about 30% lower than the cost of fossil-fuel produced product. The pay-back period was less than 5 years. Additional contacts were meanwhile also made with other lime producers in Spain, Algeria, and South Africa. It should also be remembered that that the international cement producer Cemex is part of the SOLPART consortium, and the Cemex plant in Alicante (Spain) has been selected for the industrial demonstration. No contacts outside Cemex were made.

Phosphate Calcination

L'Office Cheriflen des Phosphates (OCP) is also an associate partner in the SOLPART project. The application of solar energy seems a valid alternative since major phosphate producing countries also experience high values of DNI, Morocco being an example. OCP samples were analyzed. The average particle size is 172 μm. Heat requirements and reaction kinetics were determined by TGA and DSC. Recorded weight losses were 0.9 % around 100 °C through moisture evaporation, 2.08% between 420 and 510 °C as a result of burning C-contaminant; and 7.32% between 620 and 900 °C from the decarbonation reactions. The combustion of C generated ~ 180 kJ/kg phosphate. Preheating phosphates and fluidization air to reaction temperature consumes 719 kJ/kg phosphate. The heat for de-carbonation is 263 kJ/kg phosphate. The net heat is hence 802 kJ/kg phosphate. The required treatment time is ~45 minutes. Since SOLPART reactors operate at air velocities <0.05 m/s against ~1m/s in the current industrial phosphate calcination reactors, the heat required to preheat the air is negligible. Phosphate feed stock will be preheated by SOLPART exhausts. The solar treatment of raw phosphate will therefore require a solar energy input of maximum 300 kJ/kg phosphate, a reduction by nearly 65% in comparison with the current solution. Considering the annual average DNI-values and the duration of solar irradiance, two alternatives are being studied: either a solar reactor of ~40 MWth operated during the daytime at 480 ton/hr of raw material, or a continuous hybrid 17 MWth reactor (fossil fuel for night time and sun-lean days). Both solutions will significantly reduce the fossil fuel consumption and result in a reduced CO_2 emission of 72,000 to 84,000 ton/year. Considering both the required investment of a 40 MWth receiver-reactor, and the costs of currently consumed fuel oil and electricity, the payback period is estimated at 3 to 4.5 years.

Other Minerals

Additional experiments were conducted and industrial contacts were made with various manufacturers (clays, sand, meta-kaolin, cristobalite). With reserves of high purity clays in Europe being slowly depleted, alternative clay resources need to be exploited and imported. In analogy with the phosphate rock, these deposits contain carbonaceous impurities that need to be eliminated by thermal treatment prior to applying the clays in fabricating pipes, tiles and similar products. Since target supplies investigated are from North Africa, the use of solar calcination offers a potential for a clean and energy-friendly process. Tests are currently performed to investigate this process (650 – 750 °C), and will be reported upon.

Meta-kaolin needs de-hydroxilation (removal of chemically bound water) at a temperature of 500 to 650 °C, when the aluminosilicate structure becomes amorphous or weakly crystalline and develops a pozzolanic reactivity (possible use in grouts as a blend with lime or dolomitic lime, in pozzolanic cements and mortars, etc. Due to current shortages of high quality sand in Europe, new resources need to be developed. The Sahara desert offers this possibility, as was previously studied and demonstrated by the "Deutsches Zentrum für Luft- und Raumfart" (DLR, also SOLPART member), with the aim of replacing up to 15% of the total amount of sand in concrete products by

desert sand. Depending on the source from where the sand was obtained, it was found that different components like silt, clay, as well as various salts or sulfur compounds were present, which have a harmful effect on concrete. A thermal pre-treatment of the desert sands is required, and the use of a solar thermal kiln is investigated.

Finally, the SOLPART consortium member New Lime Development (NLD) developed a specific hybrid solar system for calcining and sintering dolomite. Initial contacts were made in Algeria for a possible 300 t/day hybrid process. Details will be made available in the presentation.

CONCLUSIONS

The solar horizontal bubbling fluidized bed concept developed within the SOLPART research project can be used as a solar receiver-reactor. The SOLPART project paves the route to applications of solar heat at up to 900°C in the mineral industry. The challenges address a multidisciplinary domain that involves particle technology, chemical engineering and solar engineering. This application offers a considerable industrial potential, as illustrated in the paper. The most demanding application is the calcination of limestone, either as pure calcite, or as 85% mix in cement raw meal. Other thermal treatments (e.g. dolomite, gypsum, phosphate rock, meta-kaolin, clays, etc.) are less demanding since occurring at a lower temperature and with an endothermic reaction heat that is significantly lower than the reaction heat of CaCO3, which is therefore considered as a relevant test case.

ACKNOWLEDGEMENTS

This work was funded both by the Beijing Advanced Innovation Center for Soft Matter Science and Engineering of the Beijing University of Chemical Technology and by the European Union's Horizon 2020 research and innovation program under grant agreement 654633, project SOLPART.

REFERENCES

1. H. Zhang, R. Dewil, J. Degrève, and J. Baeyens, Int. J. Sustain. Eng. **7**, 307 (2014).
2. D. Geldart, Powder Technol. **7**, 285 (1973).
3. D. Geldart, E.C. Abdullah, and A. Verlinden, Powder Technol. **190**, 70 (2009).
4. J. Baeyens, D. Geldart, and S.Y. Wu, Powder Technol. **71**, 71 (1992).
5. J.W. Carson, Handb. Powder Technol. **10**, 153 (2001).
6. D. Kunii and O. Levenspiel, *Fluidization Engineering*, second edi (Butterworth-Heinemann, Newton-MA (USA), 1991).
7. M. Van de Velden, J. Baeyens, and I. Boukis, Biomass and Bioenergy **32**, 128 (2008).
8. J. Baeyens, P. Cuvelier, and D. Geldart, ZEMENT-KALK-GIPS **12**, 620 (1989).
9. B. Vosteen, Die Physikalische Und Chemische Kinetik Der Thermischen Zersetzung von Kalk, Technische Hochschule Carolo-Wilhelmina zu Braunschweig, 1970.
10. H. Mikulčić, M. Vujanović, and N. Duić, J. Clean. Prod. **88**, 262 (2015).
11. J. Wuhrer, Chemie Ing. Tech. **30**, 19 (1958).
12. A. Brems, J. Baeyens, J. Beerlandt, and R. Dewil, Resour. Conserv. Recycl. **55**, 772 (2011).
13. H. Zhang, H. Benoit, I. Perez-Lopez, G. Flamant, T. Tan, and J. Baeyens, Renew. Energy **111**, 438 (2017).
14. G. Flamant, D. Gauthier, H. Benoit, J.-L. Sans, R. Garcia, B. Boissière, R. Ansart, and M. Hemati, Chem. Eng. Sci. **102**, 567 (2013).
15. H. Zhang, W. Kong, T. Tan, F. Gilles, and J. Baeyens, Sci. Rep. **7**, 10178 (2017).
16. S. Tescari, M. Neises, L. de Oliveira, M. Roeb, C. Sattler, and P. Neveu, Sol. Energy **95**, 279 (2013).
17. W. Kong, J. Baeyens, S. Li, H. Ke, T. Tan, and H. Zhang, Chem. Eng. Sci. **187**, 213 (2018).
18. G. Flamant, J. Baeyens, and H. Zhang, European Patent EP17306005 (2017).